Thin Solid Films 609 (2016) 12–18

Contents lists available at ScienceDirect

Thin Solid Films

journal homepage: www.elsevier.com/locate/tsf

Correlation of the crystal orientation and electrical properties of silicon thin films on glass crystallized by line focus diode laser

J. Yun [a,*], J. Huang [a], A. Teal [a], K. Kim [a,b], S. Varlamov [a], M.A. Green [a]

[a] School of Photovoltaic and Renewable Energy Engineering, University of New South Wales, Sydney, NSW 2052, Australia
[b] Suntech R&D Australia, Botany, NSW 2019, Australia

ARTICLE INFO

Article history:
Received 23 November 2015
Received in revised form 20 January 2016
Accepted 25 January 2016
Available online 27 January 2016

Keywords:
Crystallization
Silicon
Solar cells
Thin-films
Thin-film deposition

ABSTRACT

In this work, crystallographic orientation of polycrystalline silicon films on glass formed by continuous wave diode laser crystallization was studied. Most of the grain boundaries were coincidence lattice Σ3 twin boundaries and other types of boundaries such as, Σ6, Σ9, and Σ21 were also frequently observed. The highest photoluminescence signal and mobility were observed for a grain with (100) orientation in the normal direction. X-ray diffraction results showed the highest occupancies between 41 and 70% along the (110) orientation. However, the highest occupancies changed to (100) orientation when a 100 nm thick SiO_x capping layer was applied. Suns-Voc measurement and photoluminescence showed that higher solar cell performance is obtained from the cell crystallized with the capping layer, which is suspected from increased occupancies of (100) orientation.

© 2016 Elsevier B.V. All rights reserved.

1. Introduction

Polycrystalline silicon (poly-Si) thin film solar cells on glass, which combine the advantages of both wafer Si solar cell technology and thin-film solar cell technology, are strong candidates for next generation photovoltaics. Si, which is an abundant material, offers the advantages of nontoxicity and low cost. Poly-Si thin film solar cells consisted of a 2 μm thick solid-state crystallized thin film on borosilicate glass achieved a 10.4% photovoltaic conversion efficiency [1]. However, a high density of dislocation defects up to $1 \times 10\ cm^{-2}$ was generated during the solid-state crystallization that led to lifetime limiting recombination, which greatly reduced the open circuit voltage [2,3]. Recently, liquid phase crystallization, including continuous wave (CW) diode laser crystallization and electron beam crystallization of Si thin films on glass is reported to lead to large grains with sizes up to few tenths of mm in length [3–7]. Dislocation density was greatly reduced using this process and recent reports indicated the achievement of initial efficiency up to 11.7% [8].

Our previous findings showed that the Si films deposited above 550 °C have (110) preferential orientation before and after the laser crystallization [9]. Also, we reported that preferential orientation can be controlled using SiO_x capping layer [10]. Although the capping layer was found to have influences on crystallographic orientation of the film, its impact on solar cell performance has not been understood.

In the present work, in-depth analysis was done on microstructure and crystallographic orientation of 10 μm thick Si thin film on glass crystallized by diode laser crystallization. Also, influence of a SiO_x capping layer in terms of crystallographic orientation and electrical performance was investigated.

2. Experiment

On a 3.3 mm thick planar borosilicate glass (Schott Borofloat33) substrate with a surface area of 50 × 50 mm, SiO_x 100 nm thick barrier layer was deposited by plasma-enhanced chemical vapor deposition (PECVD) at 200–300 °C, below 1 mT with deposition rates of 5–30 nm/min. Then, the SiO_x layer was subjected to a dehydrogenation annealing step at 500 °C for 2 h under N_2 flow. 10 μm thick Si films were deposited by e-beam evaporation at 650 °C. During the deposition, *in-situ* boron doping was performed on to realize a doping concentration of boron ~$2 \times 10^{16}\ cm^{-3}$. The films were crystallized by an 808 nm continuous wave diode laser. The laser beam has a Gaussian profile with 12 mm width and 85 μm length. The laser was scanned perpendicular to the 50 mm long axis. The samples were placed on pre-heated stage at 650 °C to prevent cracks in the glass substrate during the laser scanning.

After removal of native oxide formed during the crystallization by HF dip, phosphorus dopant source (P508, Filmtronics, Inc.) was spin-coated. Subsequently, rapid thermal process (RTP) was conducted at 870 °C for 2 min. Junction depth around 500 nm was achieved and emitter sheet resistance of 300–500Ω/□ was obtained.

The crystallographic orientation is analyzed by X-ray diffraction (XRD). Receiving slit of 3–8 mm^2 was used to measure the (111),

* Corresponding author.
E-mail address: j.yun@unsw.edu.au (J. Yun).

http://dx.doi.org/10.1016/j.tsf.2016.01.048
0040-6090/© 2016 Elsevier B.V. All rights reserved.

(400), and (220) pole figures with background subtraction. The defocused errors and pole figures were corrected and calculated respectively, using the texture analysis. For EBSD (Electron Backscatter diffraction) measurement, NordlysF detector EBSD analytical system interfaced to a Carl Zeiss AURIGA® CrossBeam® Workstation is used.

PL measurement used excitation light of 465 nm, 530 nm, or 630 nm with an intensity of ~100 mW/cm^2. The infrared noise from the excitation source is removed by a short-pass filter before the sample. Any residual short wavelength excitation light after the sample is removed by a long-pass filter before the camera.

Hall measurement was conducted using the cross-type Van-der Pauw four point measurement geometry [11]. The thin film sample is etched or laser isolated into the cross pattern and electrical contacts are made beyond the distance a along each arm using a GaAl alloy. A magnetic field on the order of 1 T and current density of ~10^{-3} A/cm was used.

3. Results and discussion

3.1. Microstructure and crystallographic orientation

Large area image of the polycrystalline Si film crystallized by the diode laser at a scan speed of 40 cm/min is shown in Fig. 1 (a). Secco etch was performed in order to reveal the grain boundaries. As expected, lateral grains were formed in the scan direction. However, some grains were not formed exactly parallel to the scan direction as indicated by red arrows. Fig. 1 (b) shows the cross sectional view of the grains, which are not at right angles to the top surface. When these tilted grains converge, the grain growth in the scan direction ceases. As a result, grains of lengths ranging to several millimeters long and widths ranging to a few millimeters are grown. Longer grains in the scan direction can be realized if all the grains were tilted in the same direction or if the proportion of the grains that are at right angles to the top surface increases.

The spacing between parallel grain boundaries ranged from a few nanometers to several hundred micrometers. Electron backscatter diffraction (EBSD) mapping was carried out to characterize these boundaries. Fig. 2 shows EBSD images of resulting orientations in the scan direction, perpendicular to the scan direction, and along the surface normal direction. Corresponding charts are showing the relative frequency of each misorientation and sigma-value of CSL boundaries. Samples were crystallized with scan speed of 40 cm/min and power density of 15 kW/cm^2. In Fig. 2 (a), it can be seen that two types of parallel grains that have different orientations are alternatively formed. It is clearly shown in Fig. 2 (a) that two distinct orientations, (112) and (223) are present in the scan direction, whereas, all these grains have the same orientation of (102) in the normal direction. The sigma-value map indicates that these boundaries were Coincidence Site Lattice (CSL) Σ3 twin boundaries.

Fig. 2 (b) exhibits a fairly different situation although there are still parallel grain boundaries as in Fig. 1 (a). In this case, the grains do not have same orientation in the normal direction, instead (111) and (110) orientations are present in Fig. 2 (b). In the scan direction, all grains are distributed between all different orientations. In such boundaries, not only Σ3 boundaries are present but also Σ9 boundaries exist in the same quantity.

Fig. 2 (c) shows the case where the linear grains are not perfectly parallel to each other. The boundaries meet each other at different angles and form a triangular shape for some grains. It is very interesting that four distinct grains are located sequentially, which are marked as 1–4. It is shown that Grain 1 & 4 have (323) and (111) orientations in the scan direction and the normal direction respectively. Grain 2 & 3 have (214) orientation in the scan direction. However, Grain 2 has (103) orientation and Grain 3 has (203) orientation in the normal direction. There are Σ3, Σ6, and Σ21 CSL boundaries. Boundaries between Grain 1 and Grain 2, Grain 2 and Grain 3, and Grain 3 and Grain 4 form a Σ3 CSL boundary. Whereas, a boundary between Grain 2 and Grain 4 forms Σ6 and a boundary between Grain 1 and Grain 4 forms Σ21.

Fig. 3 is an illustration of the orientations of different grains that have been often observed in EBSD measurement. Grain 1 has (100) orientation in the normal direction. Grain 2, 3, and 4 have CSL boundaries adjacent to each other and often have (112), (111), and (110) orientations in the normal direction. Grain 5 does not contain any grain with CSL boundaries and does not usually form in as a lateral shape, rather, it forms as a round shape. Orientation of such grains is (102) and (213) in the normal direction. Similar growth behavior can be also found from polycrystalline silicon casting based on the directional growth, which exhibits (112) and (110) growing direction.

Electrical activity of the grain boundary is determined from impurity segregation or CSL type of grain boundary [12,13]. Σ3 twin boundaries were found to show a low electrical activity or no activity [12–14], therefore, they did not act as recombination sites. However, the different types of CSL boundaries can exhibit a high electrical activity by attracting minority carriers and increasing recombination.

A SiO_x capping layer is often applied prior to laser crystallization in order to control laser fluence [15], surface roughness [16], and surface energy [17]. When 100 nm thick SiO_x capping layer is applied to our

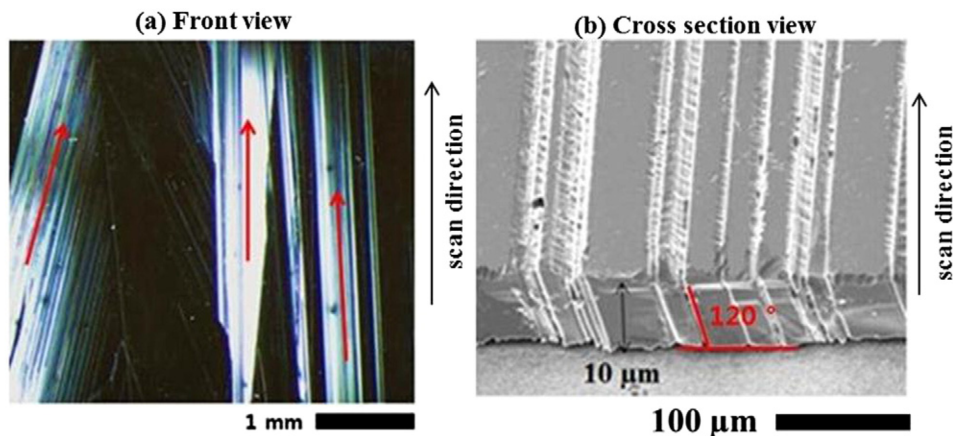

Fig. 1. Microstructure of the laser crystallized film scanned at 40 cm/min and 15 kW/cm^2. (a) Front view of the mid-horizontal area of the film (Red lines represent the direction of the grain boundaries). (b) Cross sectional view of the parallel grain boundaries by scanning electron microscopy (SEM).

Download English Version:

https://daneshyari.com/en/article/1663998

Download Persian Version:

https://daneshyari.com/article/1663998

Daneshyari.com